Electron spin resonance across the charge-ordering transition in YBaMn$_2$O$_6$

D. V. Zakharov, J. Deisenhofer, H.-A. Krug von Nidda, and A. Loidl

Experimentalphysik V, Center for Electronic Correlations and Magnetism, Institute for Physics, Augsburg University,
D-86135 Augsburg, Germany

T. Nakajima and Y. Ueda

Material Design and Characterization Laboratory, Institute for Solid State Physics, University of Tokyo,
5-1-5 Kashiwanoha, Kashiwa, Chiba 277-8581, Japan

We investigated the metal-ordered manganite system YBaMn$_2$O$_6$ using electron spin resonance (ESR) in the paramagnetic regime across the charge ordering and structural phase transition at T_{CO}=480 K and T_t =520 K, respectively. All ESR parameters exhibit jumplike changes at T_t while the charge ordering at T_{CO} manifests itself only as a weak and broad anomaly. Above T_t the ESR spin susceptibility is reduced with respect to the dc susceptibility, indicating that only the t_{2g}-core spins of Mn ions contribute to the resonance absorption. The contribution of the e_g spins is suppressed by the time scale of the polaronic hopping process of the e_g electrons. The linewidth in this regime is reminiscent of a Korringa-type relaxation behavior. In this picture the ESR properties below T_t are dominated by the slowing down of the polaronic hopping process. The charge fluctuations persist down to the temperature $T^* \approx 410$ K, below which the system can be described as a charge-ordered assembly of Mn^{3+} and Mn^{4+} spins.

I. INTRODUCTION

Quenched disorder has recently been singled out to be one of the necessary ingredients to understand the complex phase diagrams of manganite systems and the appearance of phenomena such as colossal magnetoresistance (CMR).[1–4] In most of these compounds $R_x^{3+}A_{1-x}^{2+}$MnO$_3$ with R being a rare-earth element and A being an alkaline-earth element such disorder inevitably exists due to the random distribution of R^{3+} and A^{2+} ions in the lattice. In order to sort out which of the plethora of phenomena in the phase diagrams are due to disorder and which are not, a controlled occupation of the corresponding lattice sites has to be achieved. This task has been accomplished in the case of half-substituted systems $R_{0.5}^{3+}A_{0.5}^{2+}$MnO$_3$, which could be successfully synthesized as RBaMn$_2$O$_6$, a new class of metal-ordered manganites.[5,6] In contrast to the disordered systems, in these compounds the MnO$_2$ planes are sandwiched by two types of rocksalt layers, RO and BaO, with different lattice sizes, as can be seen in Fig. 1.

The ordered compounds with R=(Y, Tb, ... , Sm) exhibit a transition from a metallic to a charge-ordered (CO) state within the paramagnetic (PM) regime at temperatures as high as T_{CO}=480 K for R=Y and an antiferromagnetic ground state. For ions with larger ionic radii R=(Nd, Pr, La) ferromagnetic ordering appears above room temperature. Indeed, it was shown that the absence of A-site disorder drastically stabilizes the CO phase and does prevent from the occurrence of magnetoresistance effects.[7] In reverse, a CMR effect of about 1000% at room temperature was found by a subtle tailoring of the CO transition via the ionic radius and introducing a sophisticated kind of disorder.

In this study we focus on YBaMn$_2$O$_6$ which exhibits a transition from a charge-ordered insulating to a metallic regime at higher temperatures within the PM regime. We investigate the spin dynamics by electron spin resonance (ESR) spectroscopy, which has been shown to be a very efficient tool to probe orbital order and charge order in various transition-metal oxides because ESR allows to directly access the spin of interest and probe its local symmetry and relaxation behavior.[8–12]

II. EXPERIMENTAL RESULTS

ESR measurements were performed in a Bruker ELEXSYS E500 CW spectrometer at X-band frequencies ($\nu \approx 9.47$ GHz) equipped with a continuous N$_2$-gas-flow cryostat in the temperature region $80 < T < 600$ K. The poly-crystalline samples were powdered and placed into quartz tubes. ESR detects the power P absorbed by the sample from the transverse magnetic microwave field as a function of the static magnetic field H. The signal-to-noise ratio of the spectra is improved by recording the derivative dP/dH using lock-in technique with field modulation.
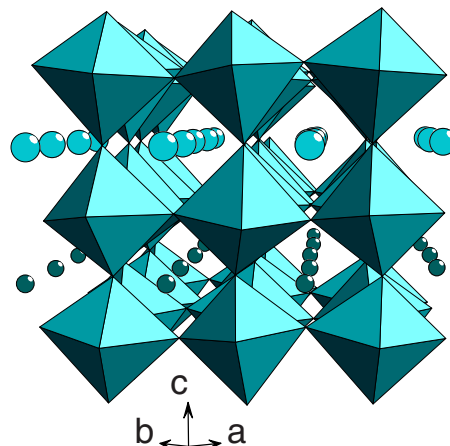

FIG. 1. (Color online) Crystal structure of YBaMn$_2$O$_6$. The Y ions (small spheres) and the Ba ions (large spheres) are arranged in alternating layers separated by MnO$_6$ octahedra.
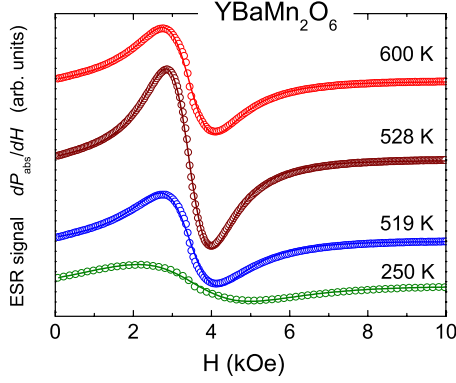
FIG. 2. (Color online) Temperature evolution of the ESR spectrum in $YBaMn_2O_6$. Solid lines represent fits using a Lorentzian line shape.

In Fig. 2 we show ESR spectra in $YBaMn_2O_6$ at different temperatures. The spectra consist of a broad exchange-narrowed resonance line, which can be very well fitted by a single Lorentzian line shape. In order to check the origin of the ESR signal we determined the absolute value of the spin susceptibility by comparison with the reference compound Gd_2BaCuO_5. It turns out that in the temperature range below about $T^* \approx 410$ K the susceptibility determined from ESR χ_{ESR} coincides with the dc susceptibility χ_{dc} (see Fig. 3). Above T^* χ_{ESR} gradually deviates from χ_{dc}. The difference reaches its maximal value at the structural transition T_t
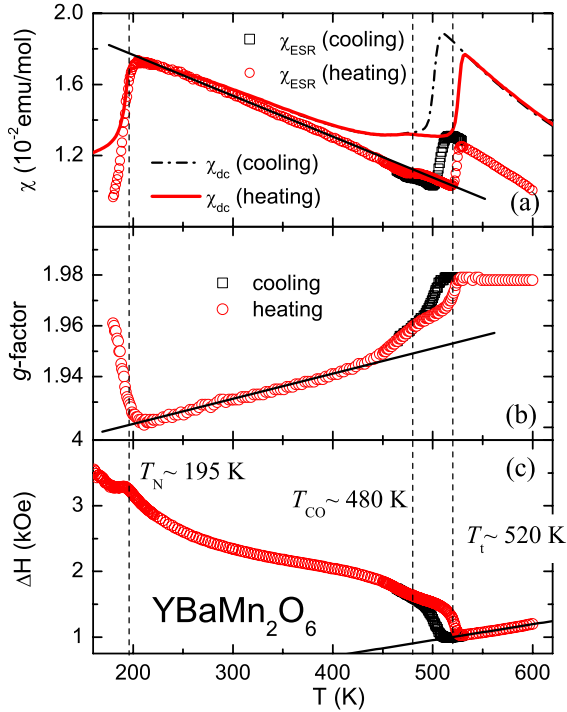

FIG. 3. (Color online) Temperature dependence of (a) the ESR spin susceptibility χ_{ESR} and the dc susceptibility χ_{dc}, (b) the effective g factor, and (c) the ESR linewidth ΔH in $YBaMn_2O_6$. The lines in the frames (a) and (b) are to guide the eyes and the line in frame (c) is a linear fit. The dashed lines indicate the transition temperatures.

$=520$ K and remains approximately constant at higher temperatures. The effective moment determined from the dc susceptibility in the high-temperature phase $T > T_t$ agrees nicely with $\mu_{dc}=6.245\mu_B$,[2] obtained when assuming that all Mn^{3+}/Mn^{4+} ions contribute to the effective moment. However, the magnetic moment determined from the ESR measurements above T_t is considerably smaller and amounts to $\mu_{ESR}=5.0(3)\mu_B$.

In Fig. 3(a) we compare the temperature dependence of the spin susceptibility χ_{ESR} obtained by ESR and the dc susceptibility χ_{dc}. In general, the differences upon heating and cooling and the features at the phase transitions are similar for χ_{ESR} and χ_{dc}. However, one can clearly see the differences in the observed effective magnetic moments in the high-temperature Curie-Weiss (CW) regime. Interestingly, this discrepancy persists throughout the two successive phase transitions at $T_{CO}=480$ K and $T_t=520$ K. The former is visible in the susceptibility as a weak and broad anomaly and has been dubbed the charge-ordering transition as the resistivity drops by more than 1 order of magnitude at 480 K.[2] The latter is a structural transition from a triclinic structure below 520 K to a monoclinic one above.[13] This structural transition shows up most dramatically in the magnetic susceptibilities as a strong increase and a subsequent renormalized CW law for $T > T_t$, while the changes in the resistivity at T_t are subtle.[2]

Let us now discuss the temperature dependence of the effective g factor [Fig. 3(b)]. In the high-temperature metallic phase $g=1.98$ is slightly below the free-electron value in accordance with the expectation for transition-metal ions with a less than half-filled d shell.[14] This value coincides with the isotropic g value observed in the orbitally disordered phase in lightly doped $La_{1-x}Sr_xMnO_3$ and in metallic manganite compounds.[15,16] Being constant above T_t, the g factor then drops at the structural transition and decreases for $T < T_t$ down to $g=1.92$ at 200 K. The transition at $T_{CO}=480$ K appears also here only as a broad anomaly in the temperature dependence. Below 200 K the g factor shows a steep increase which is due to internal fields in the vicinity of magnetic ordering at $T_N=195$ K. To check the reliability of the obtained g values, we performed ESR measurements in Q band ($\nu \approx 34$ GHz, $H_{res} \approx 12$ kOe) at several temperatures below 300 K which agreed well with the X-band measurements.

Similar to the g factor, the linewidth in $YBaMn_2O_6$ shows distinct differences between the high-temperature metallic phase and the charge-ordered state [Fig. 3(c)]. Just above T_t the linewidth exhibits its minimum value of $\Delta H=1$ kOe and increases linearly toward higher temperatures. The linewidth increases sharply at T_t and rises continuously with decreasing temperature up to 3 kOe. Again, at T_{CO} the resistivity drop gives only rise to a weak and broad anomaly. A kink is observed at the antiferromagnetic ordering temperature $T_N=195$ K.

III. DISCUSSION

As described above all ESR parameters and the dc susceptibility show sharp changes at T_t, while T_{CO} leaves its

trace only as a weak and broad anomaly. It has been pointed out by Williams *et al.*[13] that in the temperature regime $T_{CO} < T < T_t$ the system exhibits a coexistence of two phases. We believe that with the appearance of clusters of the high-temperature phase the global CO may already be broken at T_{CO}, conducting paths show up which lead to the strong drop in resistivity, but the magnetic properties are still determined by the CO regions and vary continuously with the melting of the CO phase toward higher temperatures. Only with the complete disappearance of local charge-ordered areas at the first-order structural transition at T_t the magnetic properties undergo the most drastic changes as the exchange couplings and the local coupling between t_{2g} and e_g spins become renormalized. Therefore, we will discuss our results for $T > T_t$ and $T < T_t$ separately in the following.

A. High-temperature metallic phase ($T > T_t$)

The effective magnetic moment of about $\mu_{ESR} = 5.0(3)\mu_B$ observed by ESR in the high-temperature metallic phase is reduced with respect to the dc susceptibility, which is in agreement with the value of $6.245\mu_B$ expected for all Mn^{3+} and Mn^{4+} spins. Such a behavior is astonishing especially because in prototypical manganite systems such as $La_{1-x}Sr_xMnO_3$, the observed ESR spin susceptibilities yielded effective magnetic moments, which were enhanced in comparison to the sum of all Mn^{3+}/Mn^{4+} spins.[15,16] This effect was interpreted by Shengelaya *et al.*[17,18] due to a bottlenecked spin relaxation of the exchange-coupled Mn^{3+}/Mn^{4+} spin system to the lattice.

To account for the origin of our reduced ESR susceptibility one may imagine a situation where either the Mn^{3+} subsystem or the Mn^{4+} ions participate in the resonance process. In both cases, however, an even lower effective moment is expected and, additionally, it is difficult to reasonably justify such a scenario. We think that in $YBaMn_2O_6$ the magnetic moment observed by ESR has to be compared to the magnetic moment of $5.48\mu_B$ expected if only the t_{2g}-core spins of all Mn ions are seen by ESR, i.e., all Mn ions are in a tetravalent state. If this is the case, then we have to cope with the fact that we are at odds with the textbook knowledge of a strong local Hund's coupling between the t_{2g}-core spins and the e_g electrons. Recently, Huber *et al.*[19] challenged this textbook picture and discussed the possibility that the dc susceptibility in paramagnetic manganites cannot only be understood as due to Mn^{3+}/Mn^{4+} spins, but it can equivalently be modeled by a process where the Hund's coupling between the t_{2g}-core spins ($S = 3/2$ system) and the spins residing in the e_g state ($S = 1/2$ system) is disrupted by the hopping of the e_g electrons. As a result of the thermally activated hopping the Curie constant of the system will become temperature dependent. Note that this picture can describe quantitatively the static dc susceptibility of manganite compounds including $YBaMn_2O_6$.

In the case of the dynamic susceptibility as measured by ESR, the contribution of the e_g spin system cannot be detected anymore when the hopping time becomes short compared to a Larmor period and prevents the occurrence of the precessional motion of the spin.[20] Therefore, the reduced effective moment observed by ESR can be regarded as evidence that the time scale of the electron hopping in $YBaMn_2O_6$ is much faster than the ESR measuring frequency of 10^{-10} s. Hence, we are left with the reduced χ_{ESR} and an effective moment comparable to $5.48\mu_B$ of the Mn^{4+} ions. We would like to point out that structural investigations show that all Mn lattice sites are equivalent in the high-temperature state above T_t, supporting a picture of a system built up of Mn^{4+} ions and a highly mobile polaronic e_g-electron system, which accounts for the metalliclike behavior.[13]

Such a scenario certainly has to leave its footprints in the relaxation dynamics of the spin system and, indeed, the quasilinear increase in the linewidth with temperature in the metallic regime reminds of a Korringa-type relaxation mechanism with a slope of about 2.125 Oe/K.[21] In contrast to the classical Korringa relaxation, where the localized spins are coupled to the quasifree conduction electrons, the relaxation in $YBaMn_2O_6$ must be of a more complicated nature due to the polaronic character of the electrical conductivity. It has been argued that the linewidth in such a case is also governed by the thermally activated polaron hopping and follows the temperature dependence of the conductivity.[17,18] Although a thermally activated behavior may appear as linear in a small temperature range, the present data can only support a linear fit. Additional measurements in a broader temperature range above T_t are necessary to compare and check for different models of the spin relaxation at high temperatures.

B. Charge order and charge fluctuations for $T < T_t$

As we leave the metalliclike regime for $T < T_t$ we have to be aware of the fact that χ_{ESR} is still significantly lower than χ_{dc}, but the difference is decreasing. This is an indication that the hopping frequency of the e_g electrons approaches the ESR measurements frequency $\nu \approx 10^{10}$ Hz and the e_g spins start to participate in the resonance phenomena. This slowing down of the e_g electrons corresponds to a localization process leading to a charge ordering into Mn^{3+} and Mn^{4+} states. This growing contribution of Mn^{3+} ions is certainly reflected in the behavior of the effective g factor and the linewidth.

The g factor is very sensitive to changes in the local symmetry of the spin.[20–22] Having six different Mn-O bond lengths, the MnO_6 octahedra in $YBaMn_2O_6$ are heavily distorted,[2] and one would expect the g tensor to be strongly anisotropic. Here, in the case of a polycrystalline sample, the g factor will be a statistical average of all orientations. Hence, we will have to concentrate on the information which can be obtained from the relative changes in the g factors upon temperature.

First, we want to refer to the properties of polycrystalline $La_{1-x}Sr_xMnO_3$, where a similar change in the g factor as the one arising for $T < T_t$ has been observed as a consequence of a transition into a cooperatively Jahn-Teller distorted phase.[16,23] The reason for this shift is the anisotropy arising from long-range orbital ordering of Mn^{3+} ions as it was shown in single crystals of $La_{1-x}Sr_xMnO_3$. The main parameters to describe the temperature dependence and anisotropy
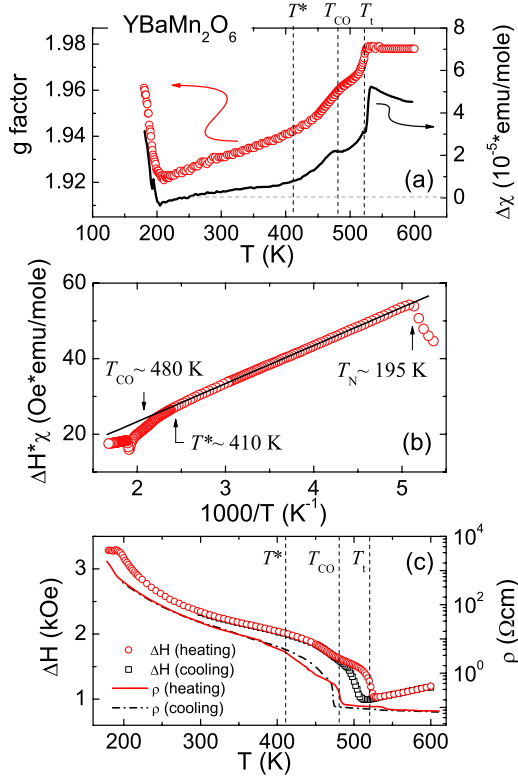
FIG. 4. (Color online) Analysis of the ESR parameters in YBaMn$_2$O$_6$. (a) Temperature dependences of the g factor and of $\Delta\chi = \chi_{dc} - \chi_{ESR}$. (b) Temperature dependence of $\Delta H\chi$ plotted vs the inverse temperature. (c) $\Delta H(T)$ compared to the temperature dependence of the resistivity on a logarithmic scale.

of the g factor were the local zero-field splitting (a measure of the distortion of the MnO$_6$ octahedra) and the susceptibility of the sample.[24,25] Clearly, in YBaMn$_2$O$_6$ the susceptibility changes dramatically and a considerable change in the local Mn-O bond lengths with temperature has been reported too.[2,13]

A direct comparison of the temperature dependencies χ_{ESR} and the g factor in Fig. 3 yields a linear behavior of both in a broad range below T_t, suggesting some correlation of the two parameters. When approaching T_{CO} and T_t, however, the g factor does not mimic the susceptibility anymore. Assuming that the relative change in the g factor toward lower temperatures is due to the increasing number of Mn^{3+}, we plot in Fig. 4(a) the g factor together with $\Delta\chi = \chi_{dc} - \chi_{ESR}$. The good agreement in the whole temperature range up to T_t seems to justify our assumptions up to now: $\Delta\chi$ and the g factor are a measure for the charge fluctuations and the charge-ordering process in our system.

It seems natural to expect the third ESR parameter, the linewidth ΔH, to reflect the localization process too.[26,27] In general, the linewidth is a measure of the relaxation of the spin system. With a growing number of Jahn-Teller active Mn^{3+} for $T < T_t$ the inhomogeneous broadening due to the zero-field splitting by the crystal field becomes stronger and consequently the ESR line broader.[8,11]

As pointed out by Huber *et al.*,[28] the temperature dependence of the linewidth in many manganites[15,29,30] can be described with the Kubo-Tomita approach[31]

$$\Delta H(T) = \frac{\chi_0(T)}{\chi_{dc}(T)} \Delta H_\infty \qquad (1)$$

as long as the systems are not too close to critical regions of magnetic and structural phase transitions. Here, $\chi_0 = C/T$ denotes the Curie susceptibility with the Curie constant $C = 13Ng^2\mu_B^2/4k_B = 4.875$ emu K/mol of the exchange-coupled Mn^{3+}/Mn^{4+} system and $\chi(T)$ is given by the measured dc susceptibility. Moreover, ΔH_∞ is a temperature-independent parameter, which is usually identified with the high-temperature limit of the ESR linewidth, if $\chi_0(T)/\chi(T) \to 1$ for $T \to \infty$. Hence, the temperature dependence of ΔH is dominated by χ_{dc} in this approximation. To check the validity of this formula we plot $\Delta H(T)\chi(T)$ versus reciprocal temperature in Fig. 4(b), which results in a linear behavior for 200 K $< T < T^* \approx 410$ K. From a linear fit we derive $\Delta H_\infty = 2.1$ kOe which is in good agreement with the values observed for other orbitally ordered phases in manganite systems, where values of 2–3 kOe have been found.[23,28,29] Astonishingly, the resistivity[2] as a direct measure of the charge-ordering process may also be compared with the linewidth in Fig. 4(c). Note that the resistivity is plotted on a logarithmic scale. The similarity of the temperature dependence encourages us to evoke the relation $\Delta H(T) \sim \ln[\rho(T)]$ between the ESR linewidth and the resistivity in the temperature range $T_N < T < T_{CO}$. To the best of our knowledge, such a correlation between the ESR linewidth and the resistivity has not been reported beforehand. Although speculative, this observation points to a strong coupling of the spin and charge degrees of freedom in this temperature range.

IV. SUMMARY

In summary, we found significant differences in the ESR properties of YBaMn$_2$O$_6$ between the high-temperature metalliclike regimes for $T > 520$ K and the regime $T < 520$ K. The ESR intensity in the high-temperature regime was found to be only due to Mn^{4+} ions in contrast to the dc susceptibility. This indicates that YBaMn$_2$O$_6$ represents a rare example of a system, where charge fluctuations take place on a time scale shorter than the typical spin relaxation and ESR measurement times. The linewidth for $T > 520$ K seems to follow a Korringa-type behavior. Toward lower temperatures the system is dominated by the slowing down of these charge fluctuations which influence the ESR absorption significantly. The ESR intensity approaches the dc susceptibility with decreasing temperature and the two curves coincide only below the temperature $T^* \approx 410$ K, which we interpret as the completion of the charge-ordering process. The temperature dependence of linewidth appears similar to the one of the resistivity on a logarithmic scale.

[1] D. Akahoshi, M. Uchida, Y. Tomioka, T. Arima, Y. Matsui, and Y. Tokura, Phys. Rev. Lett. **90**, 177203 (2003).

[2] T. Nakajima, H. Kageyama, M. Ichihara, K. Ohoyama, H. Yoshizawa, and Y. Ueda, J. Solid State Chem. **177**, 987 (2004).

[3] E. Dagotto, T. Hotta, and A. Moreo, Phys. Rep. **344**, 1 (2001).

[4] J. Deisenhofer, D. Braak, H.-A. Krug von Nidda, J. Hemberger, R. M. Eremina, V. A. Ivanshin, A. M. Balbashov, G. Jug, A. Loidl, T. Kimura, and Y. Tokura, Phys. Rev. Lett. **95**, 257202 (2005).

[5] T. Nakajima, H. Kageyama, H. Yoshizawa, and Y. Ueda, J. Phys. Soc. Jpn. **71**, 2843 (2002).

[6] A. J. Williams and J. P. Attfield, Phys. Rev. B **72**, 024436 (2005).

[7] T. Nakajima and Y. Ueda, J. Appl. Phys. **98**, 046108 (2005).

[8] B. I. Kochelaev, E. Shilova, J. Deisenhofer, H.-A. Krug von Nidda, A. Loidl, A. A. Mukhin, and A. M. Balbashov, Mod. Phys. Lett. B **17**, 459 (2003).

[9] V. A. Ivanshin, V. Yushankhai, J. Sichelschmidt, D. V. Zakharov, E. E. Kaul, and C. Geibel, Phys. Rev. B **68**, 064404 (2003); J. Magn. Magn. Mater. **272-276**, 960 (2004).

[10] D. V. Zakharov, H.-A. Krug von Nidda, J. Deisenhofer, F. Schrettle, G. Obermeier, S. Horn, and A. Loidl, Europhys. Lett. **83**, 67002 (2008).

[11] J. Deisenhofer, B. I. Kochelaev, E. Shilova, A. M. Balbashov, A. Loidl, and H.-A. Krug von Nidda, Phys. Rev. B **68**, 214427 (2003).

[12] D. V. Zakharov, D. G. Zverev, and V. V. Izotov, JETP Lett. **78**, 402 (2003).

[13] A. J. Williams, J. P. Attfield, and S. A. T. Redfern, Phys. Rev. B **72**, 184426 (2005).

[14] A. Abragam and B. Bleaney, *Electron Paramagnetic Resonance of Transition Ions* (Clarendon, Oxford, 1970).

[15] M. T. Causa, M. Tovar, A. Caneiro, F. Prado, G. Ibanez, C. A. Ramos, A. Butera, B. Alascio, X. Obradors, S. Pinol, F. Rivadulla, C. Vazquez-Vazquez, A. Lopez-Quintela, J. Rivas, Y. Tokura, and S. B. Oseroff, Phys. Rev. B **58**, 3233 (1998).

[16] V. A. Ivanshin, J. Deisenhofer, H.-A. Krug von Nidda, A. Loidl, A. A. Mukhin, A. M. Balbashov, and M. V. Eremin, Phys. Rev. B **61**, 6213 (2000).

[17] A. Shengelaya, G. M. Zhao, H. Keller, and K. A. Müller, Phys. Rev. Lett. **77**, 5296 (1996).

[18] A. Shengelaya, G.-m. Zhao, H. Keller, K. A. Müller, and B. I. Kochelaev, Phys. Rev. B **61**, 5888 (2000).

[19] D. L. Huber, D. Laura-Ccahuana, M. Tovar, and M. T. Causa, J. Magn. Magn. Mater. **310**, e604 (2007).

[20] G. E. Pake and T. L. Estle, *The Physical Principles of Electron Paramagnetic Resonance* (Benjamin, Reading, MA, 1973).

[21] S. E. Barnes, Adv. Phys. **30**, 801 (1981).

[22] D. V. Zakharov, J. Deisenhofer, H.-A. Krug von Nidda, P. Lunkenheimer, J. Hemberger, M. Hoinkis, M. Klemm, M. Sing, R. Claessen, M. V. Eremin, S. Horn, and A. Loidl, Phys. Rev. B **73**, 094452 (2006).

[23] M. Tovar, G. Alejandro, A. Butera, A. Caneiro, M. T. Causa, F. Prado, and R. D. Sánchez, Phys. Rev. B **60**, 10199 (1999).

[24] N. O. Moreno, P. G. Pagliuso, C. Rettori, J. S. Gardner, J. L. Sarrao, J. D. Thompson, D. L. Huber, J. F. Mitchell, J. J. Martinez, and S. B. Oseroff, Phys. Rev. B **63**, 174413 (2001).

[25] J. Deisenhofer, M. V. Eremin, D. V. Zakharov, V. A. Ivanshin, R. M. Eremina, H.-A. Krug von Nidda, A. A. Mukhin, A. M. Balbashov, and A. Loidl, Phys. Rev. B **65**, 104440 (2002).

[26] M. Heinrich, H.-A. Krug von Nidda, R. M. Eremina, A. Loidl, Ch. Helbig, G. Obermeier, and S. Horn, Phys. Rev. Lett. **93**, 116402 (2004).

[27] M. V. Eremin, D. V. Zakharov, R. M. Eremina, J. Deisenhofer, H.-A. Krug von Nidda, G. Obermeier, S. Horn, and A. Loidl, Phys. Rev. Lett. **96**, 027209 (2006).

[28] D. L. Huber, G. Alejandro, A. Caneiro, M. T. Causa, F. Prado, M. Tovar, and S. B. Oseroff, Phys. Rev. B **60**, 12155 (1999).

[29] J. Deisenhofer, M. Paraskevopoulos, H.-A. Krug von Nidda, and A. Loidl, Phys. Rev. B **66**, 054414 (2002).

[30] V. A. Atsarkin, V. V. Demidov, G. A. Vasneva, and K. Conder, Phys. Rev. B **63**, 092405 (2001).

[31] R. Kubo and K. Tomita, J. Phys. Soc. Jpn. **9**, 888 (1954).